

Electronic Supporting Information

Unraveling the Ultrafast Behavior of Nile Red Interacting with an Aluminum and Titanium Co-doped MCM41 Materials

Cristina Martin,¹ Boiko Cohen,¹ María Teresa Navarro,² Avelino Corma,² and
Abderrazzak Douhal*¹

¹ *Departamento de Química Física, Facultad de Ciencias Ambientales y Bioquímica, and
Inamol, Universidad de Castilla-La Mancha, Avda. Carlos III, S.N., 45071 Toledo, Spain.*

² *Instituto de Tecnología Química, UPV-CSIC, Avenida de los Naranjos s/n, 46022
Valencia, Spain.*

* corresponding author: Abderrazzak Douhal, email: abderrazzak.douhal@uclm.es

Acknowledgment: This work was supported by the MINECO and JCCM through Projects
Consolider Ingenio 2010 (CDS2009-0050), PRI-PIBIN-2011-1283, MAT2011-25472, MAT2012-
38567-C02-01, MAT2014-57646-P, PROMETEOII/2013/011 and PEII-2014-003-P.

Synthesis and characterization of X-Y-MCM41:

The synthesis gels were prepared with the following molar composition: $\text{SiO}_2:0.15 \text{ C16TAB}:0.26 \text{ TMAOH}:x\text{Al}(\text{OH})_3:y\text{Ti}(\text{C}_2\text{OH}_5)_4:24.3\text{H}_2\text{O}$, where x and y were varied between 0 and 0.067 (Table 1). In general, the TMAOH solution and the metal source were added to an aqueous solution of C16TAB. When the solution was homogenized, the silica was added. The homogeneous mixture was stirred at room temperature for 1 hour and, subsequently, is heated at 135°C for 24 hours at the autogeneous pressure in Teflon lined stainless steel autoclaves without rotation. The as-prepared X-MCM41 sample was recovered by filtration and extensively washed with distilled water (2 l/g solid) and then the material is dried at 60°C overnight. The occluded surfactant was removed by heating the sample at 813 K under a continuous flow of N_2 for 1 h, followed by 6 h treatment in a flow of air at the same temperature. The final solid presents MCM41 structure (XRD not shown). The metal content and textural properties of final solids are given in Table 1.

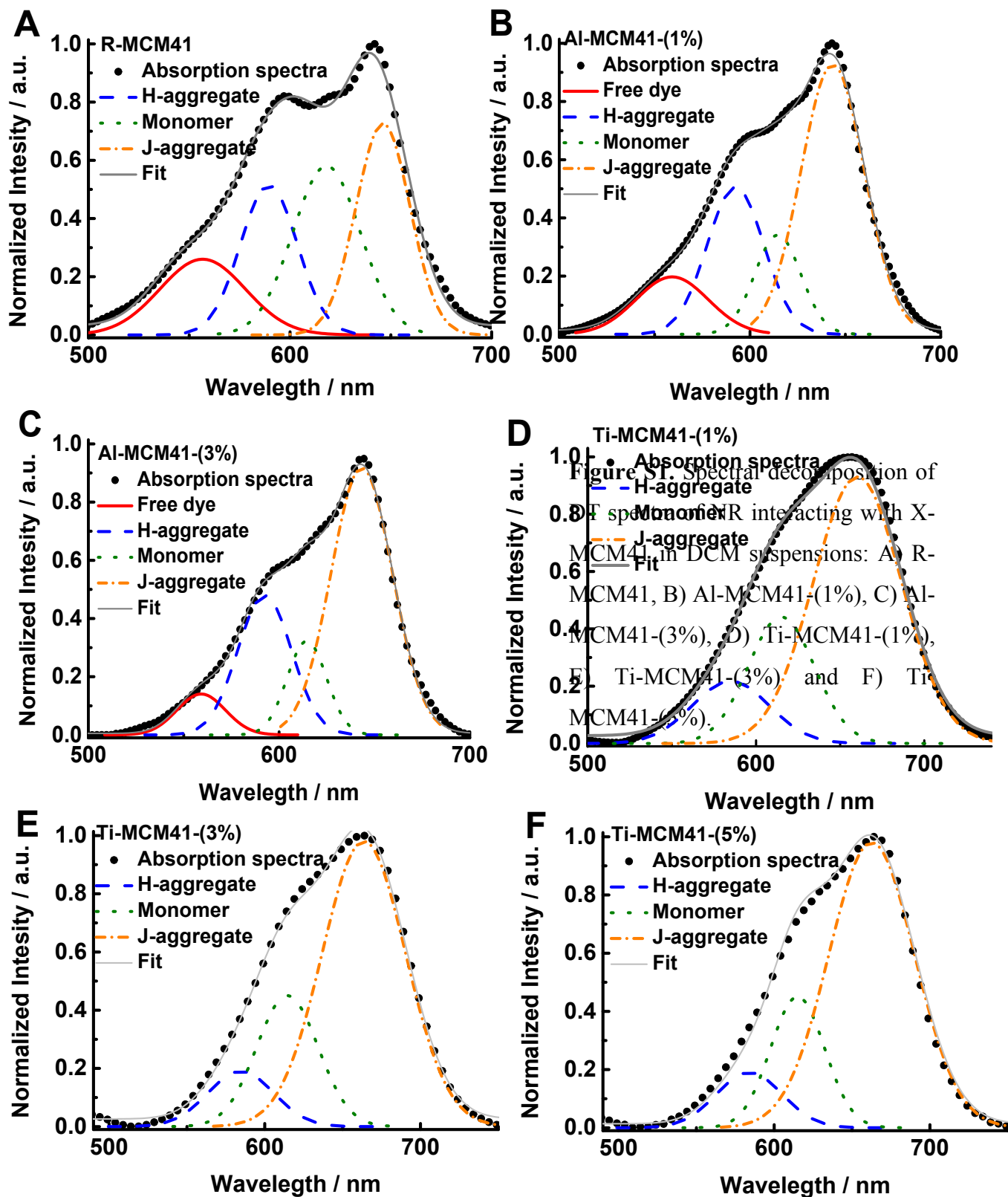
The synthesized materials were characterized by powder X-ray diffraction (XRD) with Philips X'Pert X-ray diffractometer equipped with a graphite monochromator and operating at 45 kV and 40 mA and using CuK_α radiation ($\lambda=0.1542$ nm). Chemical analyses were done using a ICP optical Emission Spectrometer Varian 715-ES, after dissolution of the solids in a $\text{HNO}_3/\text{HCl}/\text{HF}$ aqueous solution. Textural properties were determined by N_2 adsorption isotherms measured at 77 K with a Micromeritics ASAP 2020 volumetric adsorption analyzer. The Brunauer–Emmett–Teller (BET) specific surface area¹ was calculated from the nitrogen adsorption data in the relative pressure range from 0.04 to 0.2. The total pore volume² was obtained from the amount of N_2 adsorbed at a relative pressure of about 0.99. The pore diameter was evaluated using the Barret-Joyner- Halenda (BJH) method³ on the adsorption branch of the isotherms. The obtained values for each material are listed in Table 1. The composite samples in all the cases were prepared by adding 50 mg of dried MCM41 host materials to 10 ml of dichloromethane (DCM) solution containing NR (10^{-5} M) and stirring at room temperature for 15 h. The obtained material was washed several times with DCM, in order to remove weakly adsorbed dyes.

Sample	Metal		Area BET (m ² /g)	V _{total} pore (cc/g)	D _{pore} (Å)
	%Al	%Ti			
Al-MCM41	1.2	-	925	1.26	35
	3.0	-	970	1.00	35
Ti-MCM41	-	1.2	1128	0.81	35
	-	2.8	1043	1.05	35
	-	4.7	897	0.98	35
Ti-Al- MCM41	0.9	2.4	893	1.25	35
	1	1	928	1.39	35

Table S1. Values of the characteristic textural properties of X-MCM41 (X= Al, Ti, % metal contents, BET area, volume (V_{total} pore) and diameter (D_{pore}) of the pore). V_{total} pore volume and D_{pore} are the total volume pore and the diameter of the X-MCM pore, respectively,

Host	Free NR		H-aggregate		Monomer		J-aggregate		J-aggregate-2	
	λ_{Abs1} / nm	Integral Intensity (%)	λ_{Abs2} / nm	Integral Intensity (%)	λ_{Abs3} / nm	Integral Intensity (%)	λ_{Abs4} / nm	Integral Intensity (%)	λ_{Abs4} / nm	Integral Intensity (%)
R-MCM41	556	17	589	23	618	30	646	30	-	-
Al-MCM41-(1%)	559	12	593	24	614	14	643	50	-	-
Al-MCM41-(3%)	559	7	594	25	614	13	643	55	-	-
Ti-MCM41-(1%)	-	-	585	13	615	23	-	-	661	64
Ti-MCM41-(3%)	-	-	585	11	615	22	-	-	663	67
Ti-MCM41-(5%)	-	-	585	10	615	20	-	-	663	70
Ti-Al-MCM41-(1%,1%)	559	10	588	18	615	23	643	32	665	17
Ti-Al-MCM41-(3%,1%)	559	9	588	16	615	27	643	28	665	20

Table S2. Values of the maximum intensity wavelengths observed in the DT spectra of the formed species of NR upon interaction with the X-Y-MCM41 in DCM suspensions (X, Y= Al or Ti). The spectral components were obtained by a spectral deconvolution of the recorded spectrum. The spectral position error in the deconvolution analysis for the wavelength at the maximum absorption intensity ($\lambda_{\text{Abs}i}$) is about ~ 5 nm.



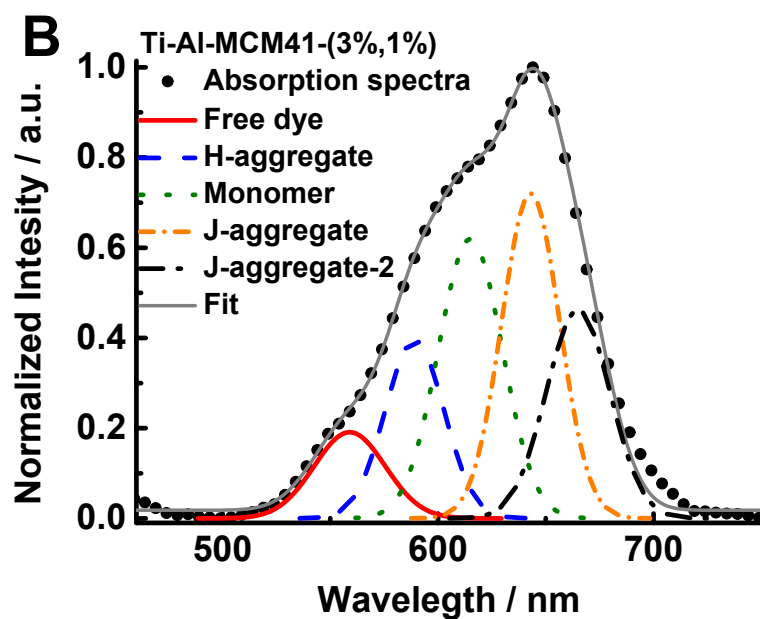
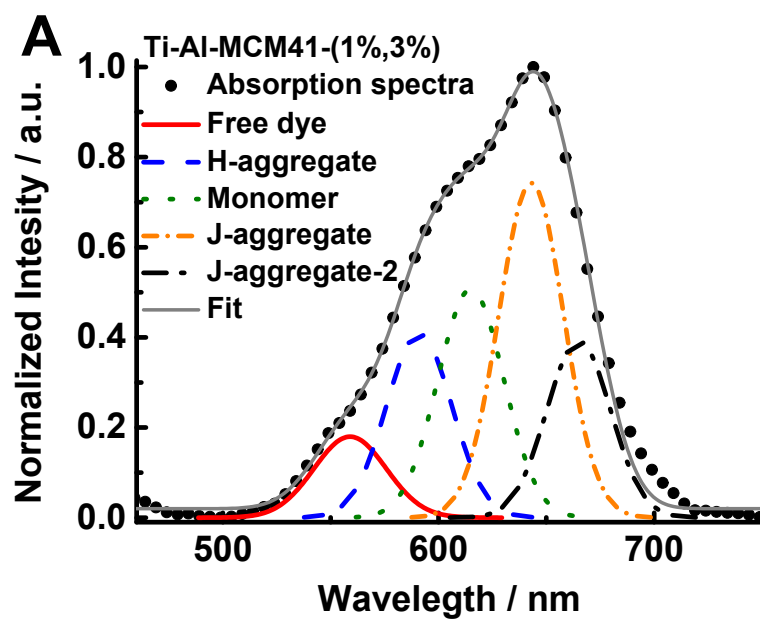


Figure S2. Spectral decomposition of DT spectra of NR interacting with X-Al-MCM41 (keeping constant the Al amount at 1%) in DCM suspensions: A) Ti-Al-MCM41-(1%,1%) and B) Ti-Al-MCM41-(3%,1%).

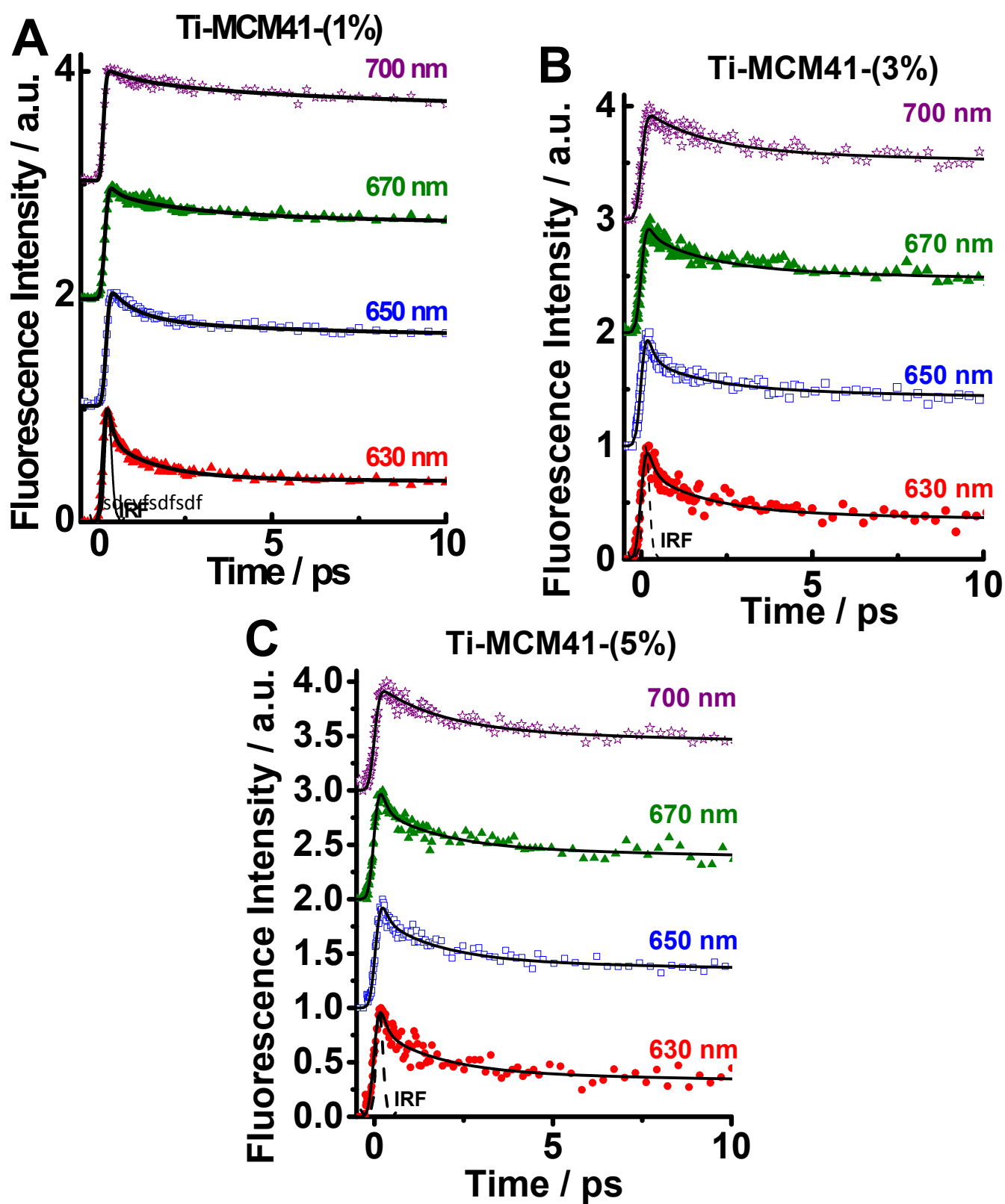


Figure S3. Magic-angle femtosecond-emission transients of NR interacting with A) Ti-MCM41-(1%), B) Ti-MCM41-(3%) and C) Ti-MCM41-(5%) in DCM suspensions at different emission wavelengths ($\lambda_{\text{ex}} = 562 \text{ nm}$). The solid lines are from the best multiexponential fits of the experimental data, and the IRF is the instrumental response function ($\sim 200 \text{ fs}$).

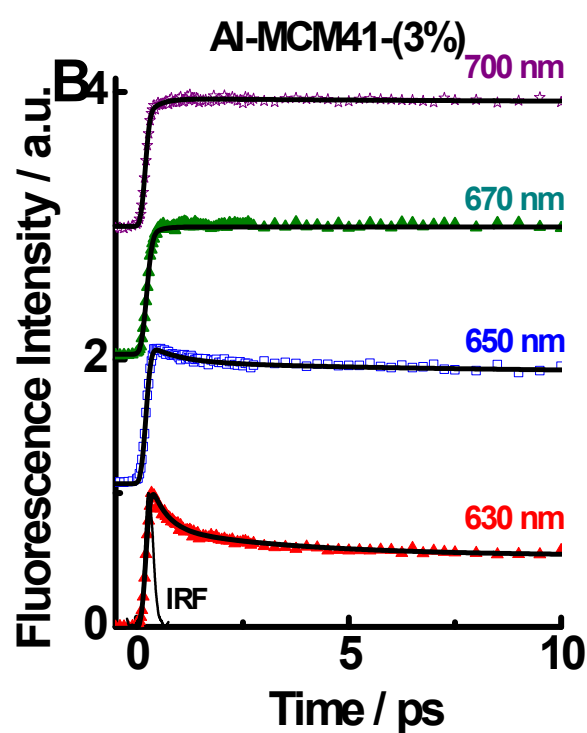
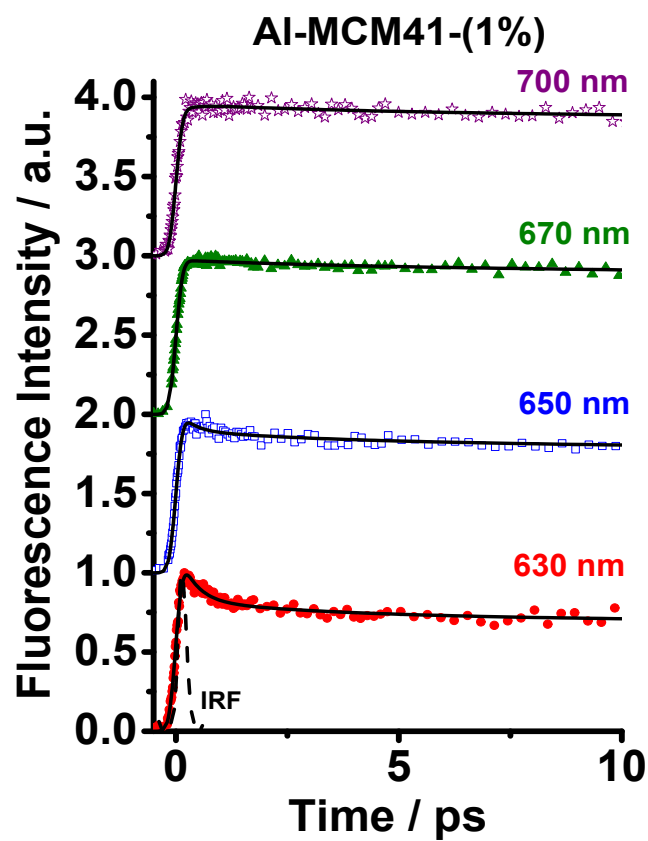


Figure S4. Magic-angle femtosecond-emission transients of NR interacting with A) AI-MCM41-(1%) and B) AI-MCM41-(3%) in DCM suspensions at different emission wavelengths ($\lambda_{\text{ex}} = 562$ nm). The solid lines are from the best multiexponential fits of the experimental data, and the IRF is the instrumental response function (~ 200 fs).

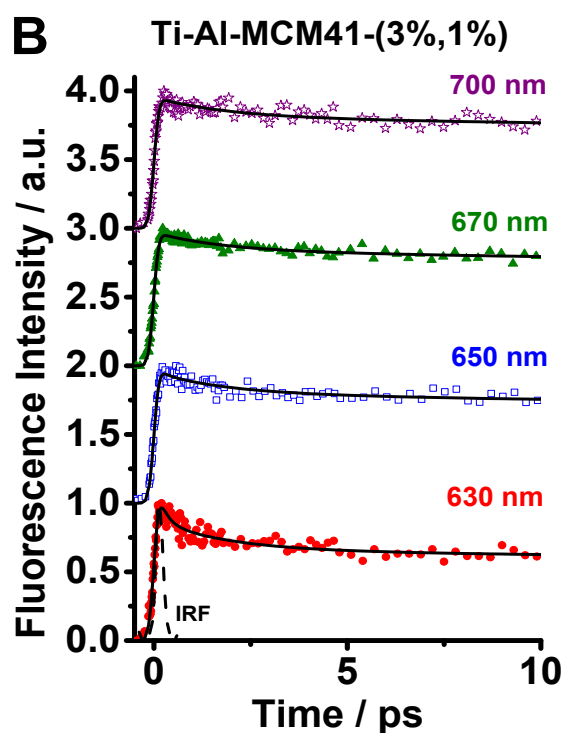
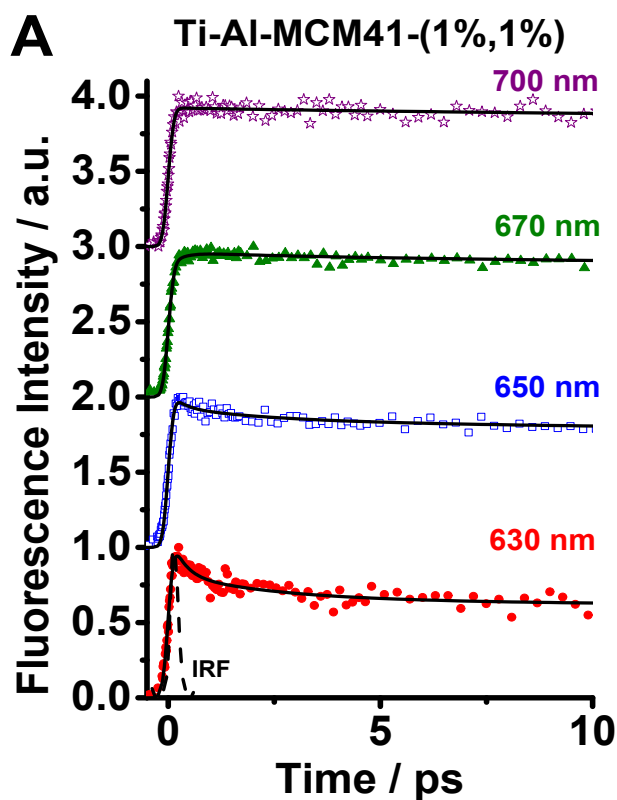


Figure S5. Magic-angle femtosecond-emission transients of NR interacting with A) Ti-Al-MCM41-(1%,1%) and B) Ti-Al-MCM41-(3%,1%) in DCM suspensions at different emission wavelengths ($\lambda_{\text{ex}} = 562 \text{ nm}$). The solid lines are from the best multiexponential fits of the experimental data, and the IRF is the instrumental response function ($\sim 200 \text{ fs}$).

References:

1. K. S. W. S. S. J. Gregg, *Adsorption, Surface Area and Porosity*, Academic Press, London, 1982.
2. K. S. W. Sing, D. H. Everett, R. A. W. Haul, L. Moscou, R. A. Pierotti, J. Rouquerol and T. Siemieniewska, Reporting Physisorption Data for Gas Solid Systems with Special Reference to the Determination of Surface-Area and Porosity (Recommendations 1984), *Pure Appl. Chem.*, 1985, **57**, 603-619.
3. E. P. Barrett, L. G. Joyner and P. P. Halenda, The Determination of Pore Volume and Area Distributions in Porous Substances. I. Computations from Nitrogen Isotherms, *J. Am. Chem. Soc.*, 1951, **73**, 373-380.